Inhibiting SSBP1 enhances ferroptosis and improves the effectiveness of sorafenib treatment for liver cancer

SAI LI[1], XINYU YANG[1], HAOXUAN GAO[1], XIUYA HU[1], DANNI WANG[1], QIQI ZHANG[1], JUAN XU[1], JIAQI ZHANG[2], LU ZHU[1,3] and ZIHAN WANG[1]

[1]Department of Pharmacology, State Key Laboratory of Experimental Hematology, Tianjin Key Laboratory of Inflammatory Biology, The Province and Ministry Co-Sponsored Collaborative Innovation Center for Medical Epigenetics, National Health Commission Key Laboratory of Hormones and Development, Chu Hsien-I Memorial Hospital and Tianjin Institute of Endocrinology, School of Basic Medical Sciences, Tianjin Medical University, Tianjin 300070, P.R. China; [2]Department of Physiology and Pathophysiology, School of Basic Medical Sciences, Tianjin Medical University, Tianjin 300070, P.R. China; [3]Department of Gynecology and Obstetrics, Tianjin Medical University General Hospital, Tianjin 300070, P.R. China

Received March 27, 2025; Accepted July 3, 2025

DOI: 10.3892/ijo.2025.5778

Abstract. Liver cancer is the third leading cause of cancer-related mortality globally, with increasing morbidity and mortality rates. Sorafenib, a multi-kinase inhibitor, is an effective first-line therapy for late-stage liver cancer. However, its effectiveness is hindered by low responsiveness, high drug resistance and significant side effects. The progression and metastasis of liver cancer are associated with alterations in mitochondrial metabolism, including mitochondrial stress responses and defects in oxidative phosphorylation, which are involved in the increased production of reactive oxygen species. Targeting mitochondrial biogenesis and bioenergetics presents a promising therapeutic strategy. Bioinformatics analysis (integrated analysis of The Cancer Genome Atlas, mitochondrial genomes, liver cancer mouse models, and bioinformatics tools) revealed that the expression of single-stranded DNA-binding protein 1 (SSBP1) was significantly elevated in liver cancer. In addition, MTT and colony formation assays showed that increased SSBP1 expression notably enhanced cell proliferation, while wound healing and Transwell assays demonstrated enhanced metastasis. Furthermore, flow cytometry, qPCR, and western blotting indicated that SSBP1 knockout impaired mitochondrial function and increased sensitivity to sorafenib, effectively attenuating cancer progression. Clinical correlation analysis demonstrated that higher SSBP1 expression was associated with poorer prognosis in patients with liver cancer. In summary, the present study identified SSBP1 as a potential driver of tumor growth and a promising prognostic biomarker and therapeutic target in liver cancer, thus providing novel insight for improving patient outcomes.

Correspondence to: Dr Zihan Wang or Professor Lu Zhu, Department of Pharmacology, State Key Laboratory of Experimental Hematology, Tianjin Key Laboratory of Inflammatory Biology, The Province and Ministry Co-Sponsored Collaborative Innovation Center for Medical Epigenetics, National Health Commission Key Laboratory of Hormones and Development, Chu Hsien-I Memorial Hospital and Tianjin Institute of Endocrinology, School of Basic Medical Sciences, Tianjin Medical University, 22 Qixiangtai Road, Heping, Tianjin 300070, P.R. China
E-mail: zihanwang@tmu.edu.cn
E-mail: zhulu@tmu.edu.cn

Key words: SSBP1, liver cancer, ferroptosis, sorafenib

Introduction

Liver cancer, the third leading cause of cancer-associated death worldwide (1), with an estimated 865,269 new liver cancer cases and 757,948 related deaths occurring worldwide in 2022, poses a significant public health challenge, especially in China, where the 5-year survival rate was 12.1% from 1990 to 2021 (2). By 2040, liver cancer may result in ~1.3 million fatalities worldwide (3,4). The pathogenesis of liver cancer is associated with chronic hepatitis infection, fatty liver disease, cirrhosis, long-term exposure to carcinogens, such as aflatoxin, and excessive alcohol consumption (5). Despite advancements in the prevention, detection and treatment of liver cancer, the majority of patients are diagnosed at advanced stages of the disease (2). Treatment is further hindered by challenges such as drug resistance and high recurrence rates.

Sorafenib, the US Food and Drug Administration-sanctioned multi-kinase inhibitor, is the sole first-line systemic therapy for liver cancer. However, its therapeutic efficacy remains limited (6). The SHARP trial (trial no. NCT00105443) demonstrated that sorafenib could extend overall survival by 2.8 months (7). In addition, the majority of patients do not experience long-term benefits due to the early onset of resistance to sorafenib. It has also been reported that ~30% of patients benefit from sorafenib, and resistance typically develops within 6 months (8). The mechanisms underlying sorafenib resistance remain poorly understood. Given the limited efficacy of the current treatment strategies, identifying

novel therapeutic targets and resolving sorafenib resistance are key for advancing liver cancer therapy.

The direct effect of sorafenib on liver cancer cells stems from ferroptosis induction rather than cell apoptosis (9,10). Ferroptosis represents a form of iron-dependent programmed cell death, which is triggered by lethal lipid peroxidation (11,12). The morphological hallmarks of ferroptosis include diminished mitochondrial cristae and atrophy (11). Both iron chelators and lipophilic antioxidants impede ferroptosis. Sensitivity to ferroptosis can be augmented by excessive iron influx, either via the interaction between transferrin and transferrin receptor or via enhanced free iron availability resulting from selective ferritin degradation, also known as ferritinophagy. Furthermore, impairments in phospholipid peroxidases, particularly glutathione peroxidase 4 (GPX4) and the upstream cystine transporter solute carrier family 7 member 11 (SLC7A11), promote susceptibility to uncontrolled lipid peroxidation and ferroptosis (13). As a result, depleted glutathione (GSH) fails to protect cells from oxidative stress and lipid peroxidation. Therefore, the accumulation of free iron and lipid peroxidation are hallmarks of ferroptosis. Sorafenib could directly inhibit SLC7A11, thereby inhibiting GSH biosynthesis (8). Therefore, targeting ferroptosis may offer a promising therapeutic strategy to overcome sorafenib resistance.

Mitochondria exert pleiotropic functions in normal physiology, including energy conversion, regulation of apoptosis, biosynthetic metabolism and cellular proliferation (14,15). They also serve a key role in stress sensing, environmental adaptation and tumorigenesis (16). Additionally, mitochondria are associated with tumor development, progression and resistance to therapy via generating reactive oxygen species (ROS), thus inducing genomic instability and modulating gene expression and signaling pathways (17-21). Alterations in mitochondrial DNA (mtDNA) are associated with cell and metabolic consequences and have been implicated in the diagnosis, prognosis and treatment of several types of tumors (22). Single-strand DNA-binding protein 1 (SSBP1), a homologue of *Escherichia coli* SSB, serves key roles in mtDNA metabolism and mtDNA replication via binding to single-stranded DNA (23,24). A study demonstrated that following DNA damage, SSBP1 promptly localizes to double-strand DNA breaks (DSBs) and is involved in DSB homology-directed repair (25). The aberrant expression of SSBP1 is associated with several pathological conditions, including organ dysfunction, neurodegenerative disease and cancer (26,27). Another study also showed that SSBP1 knockout suppresses tumor cell proliferation, thus suggesting that SSBP1 may serve as a potential therapeutic target for glioblastoma (28). However, the role of SSBP1 in liver cancer initiation, progression and sorafenib resistance remains poorly understood. Therefore, the present study aimed to investigate the effects of SSBP1 on mitochondrial function, cell proliferation, migration and ferroptosis, as well as the association between SSBP1 expression, sorafenib resistance and patient prognosis. The present study aimed to determine whether SSBP1 modulates sorafenib sensitivity via ROS-mediated ferroptosis pathways, to identify a potential therapeutic target to overcome drug resistance and improve patient outcomes.

Materials and methods

Animals. A total of six male C57BL/6J mice (age, 8-10 weeks; weight, 20-25 g) were purchased from Beijing Vital River Laboratory Animal Technology Co., Ltd. All animal experiments were performed according to international guidelines and approved by the Animal Care and Use Committee of Tianjin Medical University (approval no. TMUaMEC2024050; Tianjin, China). Animals were maintained under specific-pathogen-free conditions (21-23˚C; humidity, 60-65%; light/dark cycle, 12:12 h; free access to food/water). A diethylnitrosamine (DEN)-induced liver cancer mouse model was established as previously described (29). Briefly, 2-week-old C57BL/6J mice (weight, 8-12 g) were intraperitoneally administered 25 mg/kg body weight DEN (cat. no. W610685; Energy Chemical) (Fig. S1A). When they reached 4 weeks of age, mice were treated with weekly intraperitoneal injection of CCl_4 (5 ml/kg body weight, at a concentration of 10% in olive oil) for a total of 20 times. Mice were monitored daily for signs of distress and weighed three times/week. Abdominal distension was assessed by palpation twice/week. Behavioral parameters, including feeding efficiency and locomotor activity, were recorded daily. At 24 weeks, all mice were euthanized via inhalational exposure to CO_2 (40% chamber volume/min) in a sealed chamber, followed by confirmation of death through absence of cardiac and respiratory function for 5 min. The humane endpoints were defined as follows: i) Tumor volume >$2x10^3$ mm^3; ii) tumor diameter >20 mm; iii) rapid or continuous body weight loss >20% within 72 h; iv) tumor ulceration or necrosis leading to skin rupture or persistent exudation for >48 h and v) abdominal distension or ascites burden >10% of body weight, exhibiting an appearance analogous to that of a pregnant mouse compared with age-matched control mice. Liver tissue samples were collected following euthanasia. Cancer and adjacent paracancerous tissues were dissected, with the normal adjacent tissues sampled at a distance of ≥0.5 cm from the tumor margin to ensure clear distinction. All tissue samples were immediately snap-frozen in liquid nitrogen (-196˚C) for subsequent analyses.

Cells and transfection. Hep3B, HepG2, Huh7, Hepa1-6 and 293T cells were obtained from the American Type Culture Collection. The cells were cultured in DMEM (cat. no. MA0212; Dalian Meilun Biology Technology Co., Ltd.) supplemented with 10% fetal bovine serum (FBS; cat. no. MN012103; Mengma (Tianjin) Biotechnology Co., Ltd.) and 1% antibiotics at 37˚C under a 5% CO_2 atmosphere. A total of 20 μg lentiCRISPRv2 (cat. no. 52961; Addgene, Inc.) served as the core plasmid for constructing knockout-SSBP1 (for both mouse and human sources), and H128 pLenti-EF1α-EGFP-3FLAG-PGK-Puro (HeYuan Biotechnology Co., Ltd.) for SSBP1 overexpression. Additionally, packaging plasmids (5 μg pMD2.G and 15 μg psPAX2, second-generation lentiviral packaging plasmids) were purchased from Addgene, Inc. The plasmids [sg-SSBP1 (sg, single-guide RNA), 5'-CACCGCAAGTGACTACCTGTAATAC-3'; sg-Ssbp1 (sg, single-guide RNA), 5'-CACCGGATAGTGAAGTATACCAAAT-3'; SSBP1-Flag, forward, 5'-CCGGAATTCATGTTTCGAAGACCTGTATTAC-3' and reverse, 5'-CCTGGATCCTTCCTCTTTGCTGTCTG-3'] or control plasmids, along with packaging plasmids, were co-transfected

into 293T cells ($5x10^5$ cells/well) of a 6 well plate using polyethyleneimine (cat. no. 408727; Sigma-Aldrich). The transfection was performed according to the manufacturer's protocol at 37˚C for 6-8 h. medium was replaced with DMEM containing 10% FBS (cat. no. MN012103; Mengma (Tianjin) Biotechnology Co., Ltd.). Following incubation at 37˚C for 24 and 48 h, viral particles were collected and filtered through a 0.45 μm filter. After filtration, centrifugation was performed at 4˚C for 2 h at 60,000 x g. At one day before infection, Hep3B, HepG2, Huh7, Hepa1-6 cells were passaged into 6 well plates, and infection was performed when the cell confluency reached 70%. Before infection, fresh complete medium was added, 10-20 μl viral solution was introduced, the plate was shaken to mix evenly and then incubated at 37˚C. After 8 h, the medium was replaced with fresh complete medium. At 48 h later, puromycin (2 μg/ml) was added for selection. Following viral infection, Hep3B, HepG2, Huh7 and Hepa1-6 cells were maintained in medium containing 2 μg/ml puromycin (cat. no. P8230; Beijing Solarbio Science & Technology Co., Ltd.) to establish stable cell lines with SSBP1 knockout and SSBP1 overexpression. The successful establishment of the aforementioned cell lines was verified by western blotting.

Drugs. Sorafenib (cat. no. S1040; Selleck Chemicals) was dissolved in DMSO to a final concentration of 10 mM/ml. Hep3B cells were seeded in 6-well plates at a density of $1x10^5$ cells/well and treated with 8 μM sorafenib for 12 h at 37˚C.

Datasets and analysis. The Cancer Genome Atlas Liver Hepatocellular Carcinoma (TCGA-LIHC) datasets were retrieved from the National Cancer Institute (NCI) Genomic Data Commons (30) (portal.gdc.cancer.gov/projects/TCGA-LIHC, accession no. phs000178), while the mitochondrial localization gene set was sourced from MitoCarta3.0 (31) (https://www.broadinstitute.org/mitocarta/mitocarta30-inventory-mammalian-mitochondrial-proteins-and-pathways). Differentially expressed genes (DEGs), were identified using R language (32) (version 3.6.2; http://www.r-project.org/) with the criteria of |log2 fold change (log2FC)|>1.0 (corresponding to a more than 2-fold absolute change in expression) and adjusted P-value <0.05 (to control for false discovery rate in multiple testing), and analyzed with the Metascape online tool (33) (Metascape 3.5; https://metascape.org/gp/index.html#/main/step1). GSE14520 (34) (https://www.ncbi.nlm.nih.gov/geo/query/acc.cgi?acc=GSE14520), GSE101685 (35) (https://www.ncbi.nlm.nih.gov/geo/query/acc.cgi?acc=GSE101685), GSE151412 (36) (https://www.ncbi.nlm.nih.gov/geo/query/acc.cgi?acc=GSE151412) and GSE62813 (37) (ncbi.nlm.nih.gov/geo/query/acc.cgi?acc=GSE62813) datasets were downloaded from National Center for Biotechnology Information (NCBI) Gene Expression Omnibus (GEO) profiles (38) (https://www.ncbi.nlm.nih.gov/geo/), and the relative mRNA expression levels of SSBP1 and POLG (DNA polymerase gamma) within these cohorts were analyzed. The expression patterns of SSBP1 across TCGA in cancer were analyzed using the TIMER2.0 (39) (http://timer.cistrome.org/) and UALCAN (40) (https://ualcan.path.uab.edu/) analysis tools. The effects of SSBP1 on the survival of patients with liver cancer and those undergoing treatment with sorafenib were evaluated using the Kaplan Meier Plotter online survival analysis tool (41) (https://kmplot.com/analysis/).

Reverse transcription-quantitative (RT-qPCR). Total RNA was extracted from tumor tissue or cells using the TransZol Up RNA isolation reagent (cat. no. ET111-01-V2; TransGen Biotech Co., Ltd.) and reverse-transcribed into cDNA with the TransScriptII First Strand cDNA Synthesis SuperMix (cat. no. 11120ES60; Shanghai Yeasen Biotechnology Co., Ltd.), according to the manufacturer's instructions. qPCR analysis was performed using the SYBR Green PCR Mix (cat. no. 11200ES; Shanghai Yeasen Biotechnology Co., Ltd.) and targeted gene-specific primers (Table SI). The thermocycling conditions were as follows: Initial denaturation at 95˚C for 30 sec, followed by 40 cycles at 95˚C for 10 sec, 60˚C for 10 sec, and 60˚C for 30 sec. The relative mRNA expression levels were calculated using the ΔΔCq method (42), while β-actin served as an internal control. All primers were designed by NCBI and were synthesized by Genewiz, Inc.

To measure the copy number of mtDNA, genomic DNA extracted from liver cancer tissue or cells was quantified using qPCR. The primer sequences used are presented in Table SII.

Western blot analysis. Western blot analysis was performed as previously described (43). Briefly, total protein was extracted from tumor tissue and cells using RIPA lysis buffer (cat. no. WB3100; NCM Biotech;www.). The protein concentration was determined using a BCA kit (cat. no. CW0014S; Jiangsu CoWin Biotech Co., Ltd.) and equal amounts of protein (50 μg/lane) were separated by 10% SDS-PAGE, followed by electrotransferring onto a PVDF membrane (MilliporeSigma). Following blocking with 10% skimmed milk powder solution for 2 h at room temperature, the PVDF membrane was incubated with primary antibodies against SSBP1 (anti-rabbit; cat. no. 12212-1-AP), voltage-dependent anion channel (VDAC; anti-rabbit; cat. no. 10866-1-AP; both 1:1,000; both Proteintech Group, Inc.), Flag (anti-mouse; cat. no. F1804; Merck KGaA; 1:10,000), translocase of the outer mitochondrial membrane 20 (TOM20; anti-rabbit; cat. no. A19403; 1:5,000), glutathione peroxidase 4 (GPX4; anti-rabbit; cat. no. A11243), SLC7A11 (anti-rabbit; cat. no. A13685; both 1:1,000), and β-actin (anti-rabbit; cat. no. AC026; 1:100,000; all from ABclonal Biotech Co., Ltd.) at 4˚C overnight. Following washing with PBST (containing 0.1% Tween-20) three times (5 min each), the membrane was incubated with the corresponding Peroxidase AffiniPure™ Goat Anti-Mouse (cat. no. 115-035-003) and anti-Rabbit IgG (H+L; cat. no. 111-035-003; both 1:10,000; both Jackson ImmunoResearch Laboratories, Inc.) secondary antibodies at room temperature for 1.5 h. The membrane was washed with PBST three times and the immunoreactive signals were detected using the ECL Western Blotting Detection Reagent (cat. no. CW0049M; Jiangsu CoWin Biotech Co., Ltd.). The protein bands were scanned using the MiniChemi 610 chemiluminescence imaging system (SinSage Technology, Co., Ltd.) and relative intensity was semi-quantified by ImageJ software (ImageJ 2.0; National Institutes of Health). β-actin served as an endogenous control.

Cell viability assay. Cell viability was assessed using MTT reagent (cat. no. M8180; Beijing Solarbio Science &

Technology Co., Ltd.), as previously described (44). Briefly, liver cancer cells were plated into 96 well plates at a density of $3x10^3$ cells/well and incubated either in the presence or absence of sorafenib (8 μM). Following incubation at 37˚C for 24, 48, and 72 h, respectively the culture medium was replaced with 100 μl MTT reagent (0.5 mg/ml), followed by incubation for 4 h at 37˚C. Then, the purple formazan was dissolved in dimethyl sulfoxide (DMSO). Absorbance at a wavelength of 490 nm was measured using a microplate reader (45).

Colony formation assay. Liver cancer cells were seeded into 6-well plates at a density of $1x10^3$ cells/well in the presence or absence of sorafenib (2.5 μM) at 37˚C for ~2 weeks. Cells were washed with PBS, fixed with 4% paraformaldehyde for 20 min, and stained with 0.1% crystal violet solution (cat. no. G1064; Beijing Solarbio Science & Technology Co., Ltd.) for 30 min, both at room temperature. The colonies (>50 cells) were counted using ImageJ software (ImageJ 2.0; National Institutes of Health) and images were captured under a light microscope (magnification, x40).

Transwell assay. The migration of liver cancer cells were assessed using 24 well Transwell chambers. The upper and lower culture compartments were separated by polycarbonate membranes with 8 μm pores (Corning, Inc.). The bottom chamber was filled with DMEM (cat. no. MA0212; Dalian Meilun Biology Technology Co., Ltd.) supplemented with 20% FBS (cat. no. MN012103; Mengma (Tianjin) Biotechnology Co., Ltd.) as a chemoattractant. A total of $5x10^4$ cells in serum-free DMEM (were seeded into the upper chamber and incubated at 37˚C for 48 h in a humidified incubator with 5% CO_2. The cells that migrated to the underside of the membrane were stained with 0.1% crystal violet solution (cat. no. G1064; Beijing Solarbio Science & Technology Co., Ltd.) for 15 min at room temperature and images were captured under a light microscope (magnification, x40).

Wound healing assay. Liver cancer cells (Hep3B and Hepa1-6 cells) were cultured in a 6 well plate until ~100% confluence and a scratch was made. Following washing with PBS to remove detached cells, cells were then cultured under serum-free conditions for 24 h. Images were captured under a light microscope at 0 and 24 h to record the changes in wound width (magnification, x40). Wound distance was expressed as ratio to the initial distance at 0 h.

Immunofluorescence staining. Mitochondrial morphology was evaluated using the MitoTracker®-Red kit (cat. no. C1035; Beyotime Institute of Biotechnology), according to the manufacturer's instructions. Briefly, liver cancer cells cultured in cell chambers at 37˚C were treated in the presence or absence of sorafenib (8 μM, 12 h at 37˚C). Following washing with PBS, cells were incubated in serum-free DMEM (cat. no. MA0212; Dalian Meilun Biology Technology Co., Ltd.) supplemented with Mito-Tracker Red CMXRos (1:1,000) for 30 min at 37˚C. After washing with PBS, 1 ml serum-free medium was added to the cell chamber. A total of ≥8 randomly selected fields/sample were observed under a laser confocal scanning microscope (LSM-800; Carl Zeiss AG).

Mitochondrial mass determination. Following treatment with sorafenib (8 μM, 12 h at 37˚C), cells were harvested and centrifuged at 300 x g for 5 min at room temperature. Following washing with PBS three times, cells were incubated with the MitoTracker®-Red probe for 30 min at 37˚C. Cells were washed three times with PBS and analyzed using a 579 nm channel flow cytometer (BD FACSVerse; BD Biosciences). Data analysis was performed using FlowJo software (version 10.8.1; Tree Star, Inc.).

ROS analysis. ROS levels were measured using a DCFH-DA assay (cat. no. S0035S; Beyotime Institute of Biotechnology), according to the manufacturer's instructions. Liver cancer cells were seeded into 6 well plates at a density of $1x10^5$ cells per well and treated in the presence or absence of sorafenib (8 μM) at 37˚C for 12 h. Cells were washed with PBS three times and the fluorescence intensity was measured using a microplate reader, as previously described (44). A total of $1x10^4$ cells/sample were analyzed on a BD FACSVerse flow cytometer (BD Biosciences) using an argon-ion laser (15 mW) and an incident beam at 488 nm. Data analysis was performed using FlowJo software (version 10.8.1; Tree Star, Inc.).

JC-1 assay. Mitochondrial membrane potential (MMP) was measured using a JC-1 assay kit (cat. no. C2003S; Beyotime Institute of Biotechnology), according to the manufacturer's instructions. Hep3B cells were collected following centrifugation at 600 x g for 4 min at room temperature and washed twice with PBS. Cells were incubated with the JC-1 dye in the dark at 37˚C for 20 min. Following gently washing with PBS twice, the cells were analyzed using a BD FACSVerse flow cytometer (BD Biosciences) to detect aggregates and monomers. Data analysis was performed using FlowJo software (version 10.8.1; Tree Star, Inc.). MMP was calculated as the ratio of the fluorescence intensity of aggregates to that of monomers.

Cell death assay. Following centrifugation at 600 x g for 5 min at room temperature, $5x10^5$ Hep3B cells were collected and washed twice with PBS. The cells were re-suspended in PBS and stained with propidium iodide and Annexin (cat. no. C1067S; Beyotime Institute of Biotechnology) in the dark for 20 min. Cells were washed with PBS and $1x10^4$ cells/sample were analyzed on a BD FACSVerse flow cytometer (BD Biosciences) equipped with a 15 mW argon-ion laser and an incident beam at 488 nm. Data analysis was performed using FlowJo software (version 10.8.1; Tree Star, Inc.). Cell death was calculated as the percentage of cells positive for propidium iodide fluorescence (46).

Detection of lipid peroxidation. C11-BODIPY$^{581/591}$ (5 μM; cat. no. D3861; Thermo Fisher Scientific, Inc.) was used to measure lipid ROS levels. Hep3B cells seeded into glass-bottom cell culture dishes at a density of $2x10^5$ cells/ml, were treated with sorafenib (8 μM, 12 h at 37˚C) and incubated with C11-BODIPY$^{581/591}$ for 30 min at room temperature. Following washing with PBS three times, ≥50 cells/group were observed under a confocal microscope (Carl Zeiss AG) and the fluorescence intensity was measured using ImageJ software (ImageJ 2.0; National Institutes of Health). FITC/PE ratio was

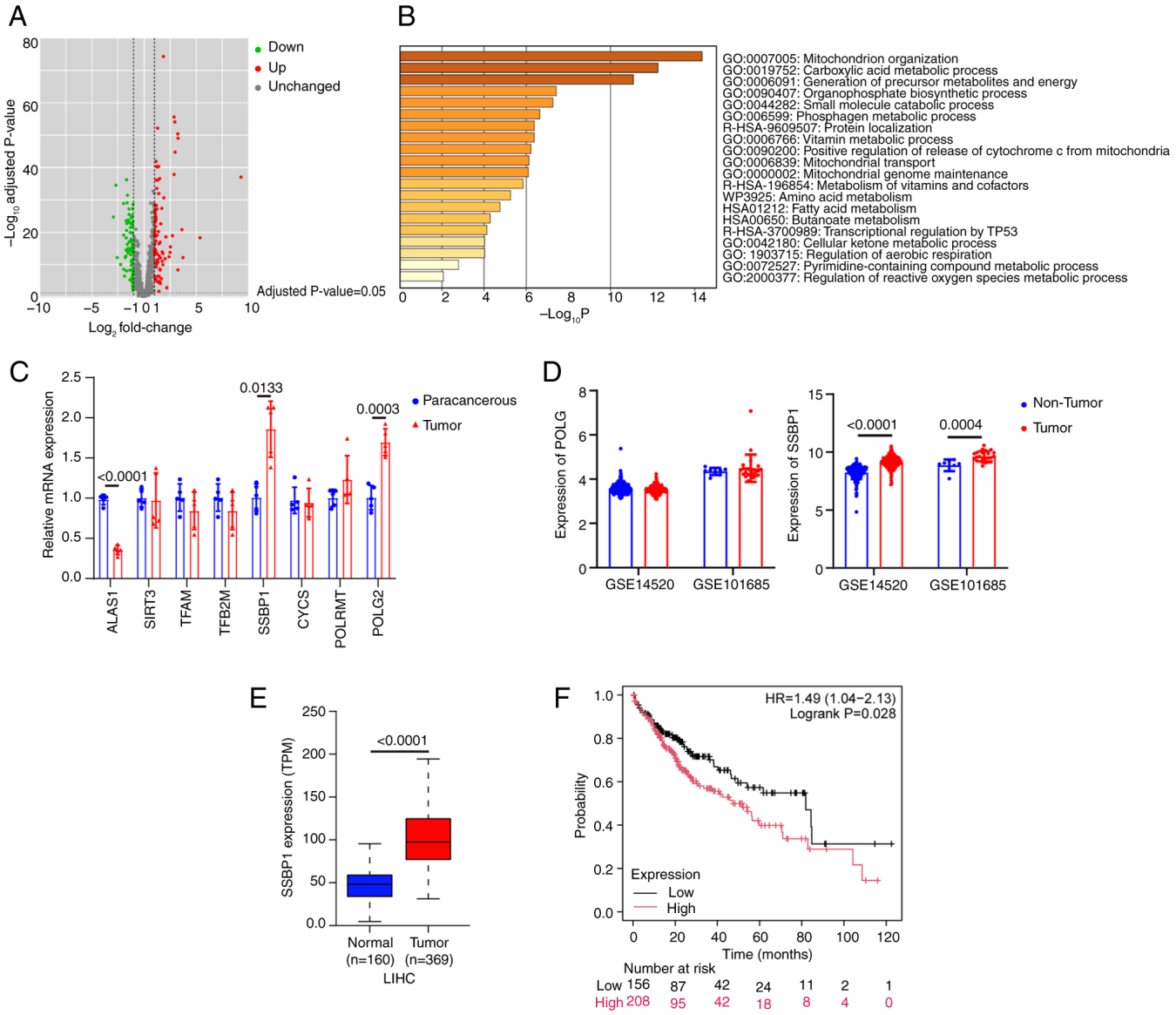

Figure 1. Integrated analysis of the expression of SSBP1 in liver cancer. (A) Distribution of differential gene expression levels after mapping mitochondrial-located genes (MitoCarta3.0 list) onto the TCGA-LIHC dataset. (B) Enrichment analysis using the R language. The gene sets ranking at the top were predominantly implicated in mitochondrial organization and biogenesis. (C) mRNA levels of mitochondrial biogenesis genes (including ALAS1, SIRT3, TFAM, TFB2M, SSBP1, CYCS, POLRMT and POLG) in liver cancer and paracancerous tissue (n=5). (D) Expression profiles of POLG and SSBP1 in patients with liver cancer and corresponding controls derived from the GSE14520 (tumor, n=225; non-tumor, n=220) and GSE101685 datasets. (tumor, n=24; non-tumor, n=8). (E) Transcriptional expression levels of SSBP1 in the TCGA-LIHC dataset. (F) Association between SSBP1 expression and the prognosis of liver cancer in the overall population (n=364) using the Kaplan Meier Plotter online survival analysis tool. SSBP1, single-stranded DNA binding protein 1; TCGA-LIHC, The Cancer Genome Atlas liver hepatocellular carcinoma; ALAS1, aminolevulinic acid synthase 1; SIRT3, sirtuin 3; TFAM, transcription factor A, mitochondrial; TFB2M, transcription factor B2, mitochondrial; CYCS, cytochrome c, somatic; POLRMT, RNA polymerase mitochondrial; POLG, DNA polymerase γ; TPM, transcripts per million.

used to determine lipid oxidation, and the mean ratio of each group was normalized to that of the control.

Statistical analysis. All statistical analyses were performed with SPSS software (version 26.0; IBM Corp.). All data are expressed as the mean ± SD, and all experiments were repeated at least three times. Unpaired two-tailed Student's t-test was used for comparisons between two groups when data passed normality and equal variance test; otherwise, the Mann-Whitney test was used. For data that were normally distributed containing >2 groups, one-way ANOVA was used followed by Tukey's comparison post hoc test. P<0.05 was considered to indicate a statistically significant difference.

Results

High SSBP1 expression is associated with the progression and poor prognosis of liver cancer. Among all mitochondrial-localized genes, 225 DEGs were identified between liver cancer and normal tissue, including 85 up and 170 downregulated genes (Fig. 1A). To determine the main functions of DEGs, the Metascape online tool was utilized. The analysis revealed that the DEGs were primarily enriched in

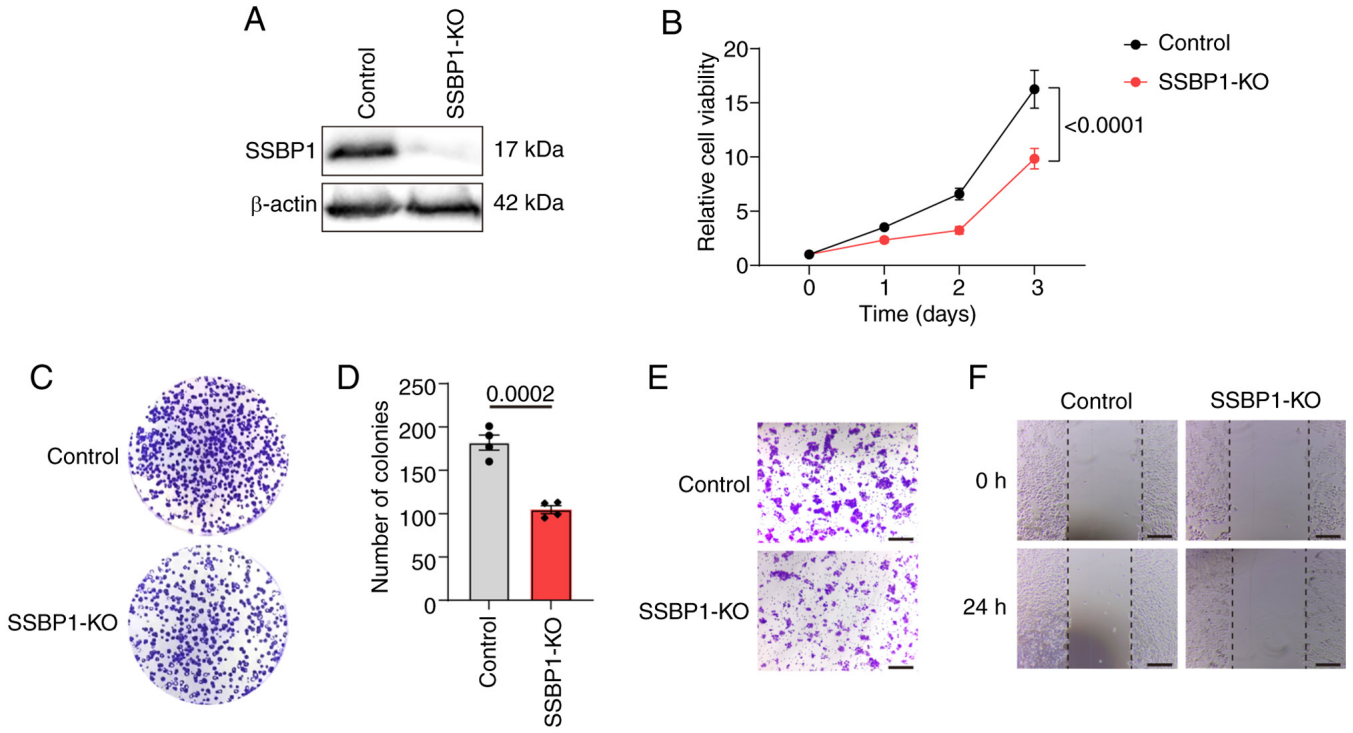

Figure 2. Knockout of SSBP1 in Hep3B cells inhibits the proliferation and migratory capacity of liver cancer cells. (A) SSBP1 expression in control and SSBP1-KO Hep3B cells. (B) MTT assay showed the relative viability of control and SSBP1-KO Hep3B cells (n=10). (C) Representative colony formation plots showing the proliferation capacity of Hep3B cells with SSBP1 KO. (D) Colony formation capacity (n=4). (E) Migratory capacity of control and SSBP1-KO Hep3B cells was examined by Transwell assay. (F) Wound healing assay was used to determine the migratory capacity of Hep3B cells with SSBP1 deficiency. Scale bar, 200 μm. Magnification, x40. SSBP1, single-stranded DNA binding protein 1; SSBP1-KO, (single-stranded DNA binding protein 1) knockout.

'mitochondrion organization' (Fig. 1B). Among 17 genes involved in mitochondrial biogenesis, eight genes, namely ALAS1, SIRT3, TFAM, TFB2M, SSBP1, CYCS, POLRMT and POLG, were significantly associated with liver cancer phenotypes within the TCGA-LIHC datasets (data not shown). A DEN-induced liver cancer mouse model was established and RT-qPCR showed that only SSBP1 and POLG2 were upregulated, while ALAS1 was significantly downregulated in tumors cells (Fig. 1C). However, in the GEO datasets, the expression of SSBP1, but not POLG, was markedly increased in liver cancer tissues compared with adjacent non-cancerous tissue (Fig. 1D). SSBP1 was upregulated in numerous types of cancer tissues compared with normal tissue (Fig. S1B and C), thus suggesting that SSBP1 could serve a key role in cancer, particularly in liver cancer (Fig. 1E). Kaplan-Meier survival analysis revealed that high SSBP1 expression was associated with poor prognosis in liver cancer (Fig. 1F). Collectively, SSBP1 may be a potential biomarker for the diagnosis and prognosis of liver cancer.

SSBP1 knockout inhibits liver cancer cell proliferation and migration capacity. To investigate the effect of SSBP1 on the growth and tumorigenesis of liver cancer, SSBP1 was knocked out using independent lentiviral sgRNA. Western blot analysis demonstrated that SSBP1 was successfully knocked out in the liver cancer cell lines (Figs. 2A and S2A, G and J). MTT assay was employed to monitor cell proliferation at 24 h intervals. Proliferation capacity of SSBP1-knockout Hep3B cells was notably decreased (Fig. 2B). Similarly, the number of colonies formed by SSBP1-knockout Hep3B cells was significantly decreased compared with control cells, consistent with the reduced proliferation capacity observed in the MTT assay (Fig. 2C and D). To explore the effect of SSBP1 on liver cancer cell migration, a Transwell assay was performed. The loss of SSBP1 markedly decreased the migration of Hep3B cells compared with the control group (Fig. 2E). Additionally, wound healing assay was utilized to assess the migration ability of SSBP1-knockout Hep3B cells. SSBP1 knockout significantly impaired the motility of Hep3B cells compared with the control (Fig. 2F). The same results were observed in Hepa1-6 (Fig. S2B-F), HepG2 (Fig. S2H and I) and Huh7 cells (Fig. S2K and L).

SSBP1 overexpression promotes liver cancer cell proliferation and migration capacity. As previously described, SSBP1 upregulation is associated with most types of cancers (28). Therefore, the role of SSBP1 in promoting liver cancer growth was investigated. Flag-tagged SSBP1 was overexpressed in liver cancer cell lines using a lentiviral system and SSBP1 overexpression was validated using western blot analysis (Figs. 3A and S3A). Compared with the control, the proliferative capacity of SSBP1-overexpressing Hep3B cells was significantly enhanced (Fig. 3B). SSBP1 overexpression promoted the colony formation capacity of Hep3B cells (Fig. 3C and D). Transwell migration and wound healing assays demonstrated that SSBP1 overexpression enhanced the migration potential of liver cancer cells (Fig. 3E and F). The same results were also obtained in HepG2 cells (Fig. S3B and C).

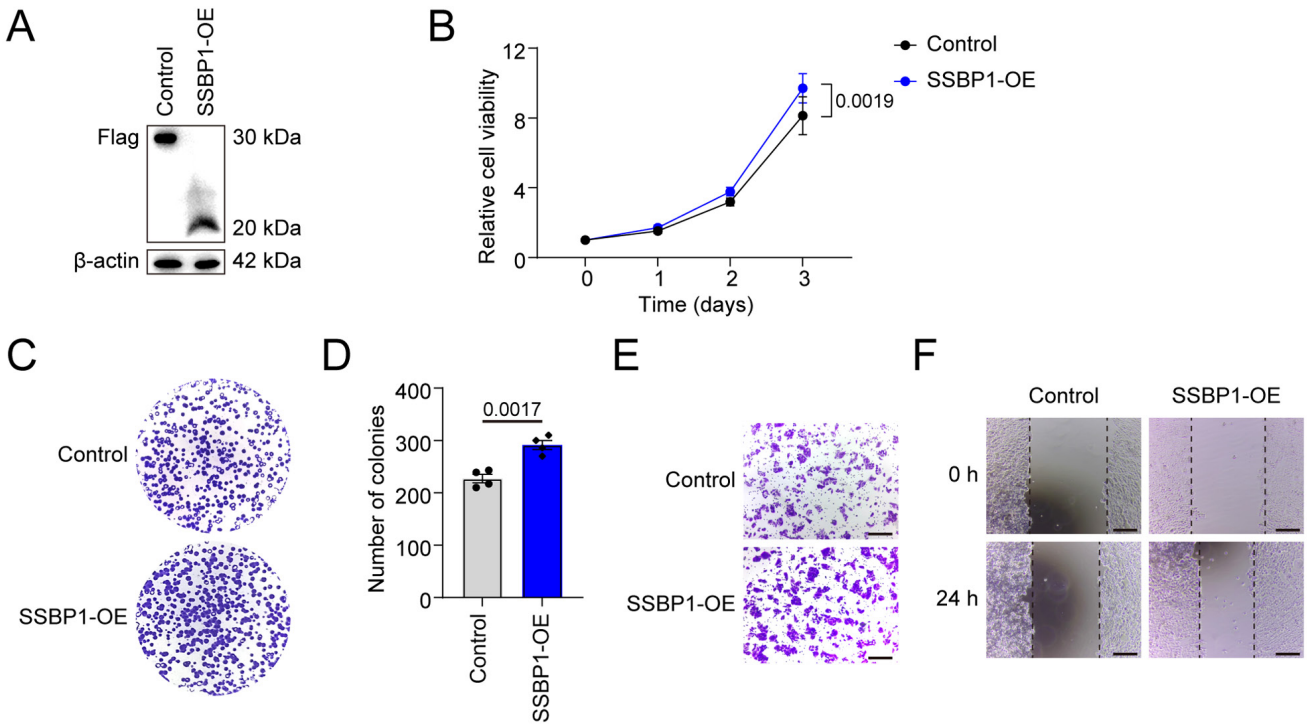

Figure 3. SSBP1-OE enhances proliferation and migratory capacity of liver cancer cells. (A) Representative bands of control and SSBP1-OE Hep3B cells to validate the effect by Western blotting. Flag signals represent fusion proteins detected by anti-Flag antibody. Control vector-transfected cells were used as negative controls to confirm specific expression of the fusion protein. (B) Viability of control and SSBP1-OE Hep3B cells (n=10). (C) Representative colony formation plots showing the proliferation capacity of Hep3B cells with SSBP1 OE. (D) Colony formation capacity (n=4). (E) Migratory capacity of control and SSBP1-OE Hep3B cells was examined by Transwell assay. (F) Wound healing assay was used to determine the migratory capacity of Hep3B cells with SSBP1 OE. Scale bar, 200 μm. Magnification, x40. SSBP1-OE, (single-stranded DNA binding protein 1) overexpression.

SSBP1 knockout inhibits mitochondrial function. SSBP1 is a key mitochondrial protein; its abnormal regulation affects mtDNA content, eventually leading to alterations in mitochondrial function (27). mtDNA copy number was elevated in liver cancer tissue (Fig. 4A). Concurrently, *SSBP1* knockout in liver cancer cells decreased the number of mitochondria while increasing their migration towards the nucleus (Fig. 4B and C). Additionally, the mtDNA copy number was decreased (Fig. 4D). Western blot analysis indicated that SSBP1 knockout diminished the expression of mitochondria-related proteins (Fig. 4E). As mitochondria serve as the primary source of cellular ROS generation (47), the accumulation of mitochondrial ROS in Hep3B cells was evaluated. A significant increase in mitochondrial ROS accumulation and a marked decrease in MMP were observed in SSBP1-deficient cells (Fig. 4F-I). These results suggested that SSBP1 knockout promoted mitochondrial damage in liver cancer cells.

SSBP1 knockout triggers ferroptosis in liver cancer cells. As aforementioned, the relative cell viability was significantly decreased by SSBP1 deficiency. Therefore, the present study aimed to investigate whether, in addition to impaired proliferation, cell death also occurred. Flow cytometry showed that SSBP1 deletion significantly increased the percentage of dead cells compared with control cells (Fig. 5A-B). Among the various types of cell death, ferroptosis is involved in the genesis and progression of liver cancer, with mitochondria, where SSBP1 is located and which are crucial energy-supplying organelles, serving a key role in this process (27-29,44,48). Therefore, C11-BODIPY fluorescence staining was employed to determine the extent of ferroptosis, and the results revealed an increase in lipid peroxidation in SSBP1-knockout Hep3B cells, confirming enhanced ferroptosis (Fig. 5C-F). Consistently, quantitative analysis showed that antioxidant genes (e.g., GPX4, SLC7A11) were downregulated at both protein and mRNA levels in SSBP1-deficient cells (Fig. 5G and H), demonstrating that SSBP1 regulates liver cancer progression via modulating ferroptosis. The same results were also observed in HepG2 (Fig. S4A and B) and Hepa1-6 cells (Fig. S4C).

SSBP1 knockout enhances the sensitivity of liver cancer cells to sorafenib. Based on the dual role of sorafenib as both a tumor suppressor and inducer of ferroptosis in liver cancer (8), the present study explored the effect of SSBP1 on sorafenib treatment. GEO datasets showed that when liver cancer cells were treated with sorafenib, the expression of SSBP1 notably decreased (Fig. S5A), whereas SSBP1 was upregulated in sorafenib-resistant cells compared with sorafenib-sensitive cells (Fig. S5B). In addition, high SSBP1 expression was associated with poor prognosis in sorafenib-treated liver cancer (Fig. S5C). Therefore, Hep3B cells were treated with sorafenib, and western blot analysis showed that SSBP1 was markedly downregulated in these cells (Fig. 6A). SSBP1 knockout enhanced sorafenib-induced inhibition of clonogenicity and growth inhibition (Fig. 6B-D). Subsequently, the

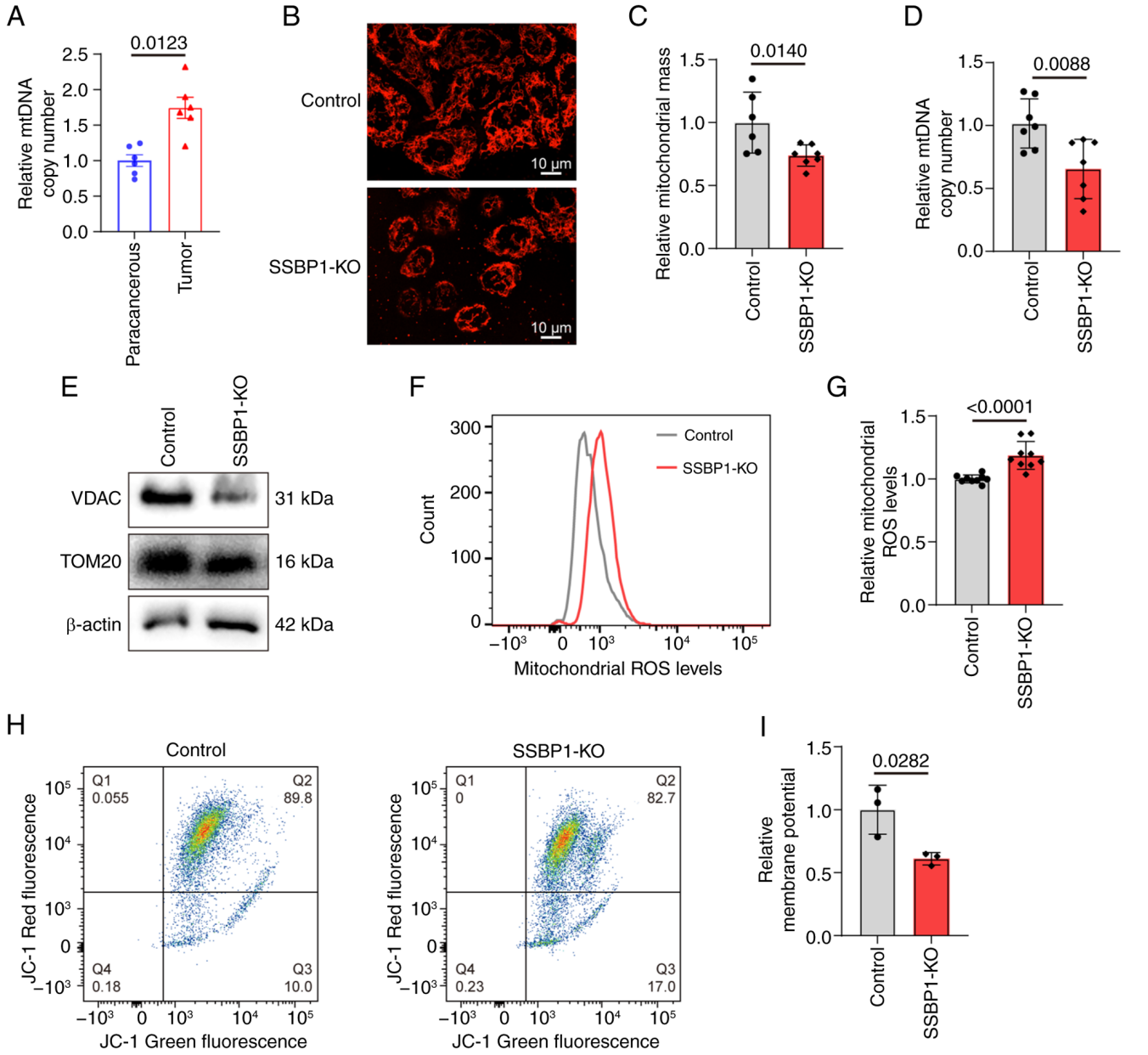

Figure 4. SSBP1 deficiency inhibits mitochondrial function. (A) qPCR was used to analyze the mtDNA copy number of liver cancer and paracancerous tissue (n=6). (B) Immunofluorescence was performed to detect the mitochondrial morphology in Hep3B cells following *SSBP1* KO. Scale bar, 10 μm. Magnification, x630. (C) Flow cytometry was employed to analyze the mitochondrial mass of control and SSBP1-KO Hep3B cells (n=6-7). (D) qPCR was used to analyze the mtDNA copy number of control and SSBP1-KO Hep3B cells (n=7). (E) Expression of mitochondrial proteins in control and SSBP1-KO Hep3B cells. (F) Flow cytometry was employed to analyze (G) levels of ROS of control and SSBP1-KO Hep3B cells (n=9). (H) Flow cytometry was applied to analyze (I) MMP of control and SSBP1-KO Hep3B cells (n=3). q, Quantitative; KO, SSBP1 (single-stranded DNA binding protein 1) knockout; mtDNA, mitochondrial DNA; VDAC, Voltage-Dependent Anion Channel; TOM20, Translocase of the Outer Mitochondrial Membrane 20; ROS, Reactive Oxygen Species.

effect of SSBP1 deficiency on sorafenib treatment in liver cancer was assessed. Following SSBP1 knockout, the mtDNA copy number and mitochondrial mass of liver cancer cells were markedly decreased following treatment with sorafenib (Fig. 6E-G). In addition, MitoTracker staining indicated that mitochondrial fragmentation was enhanced and mitochondria migrated closer to the nuclear periphery in SSBP1-knockout liver cancer cells (Fig. 6E). Furthermore, treatment of SSBP1-knockout liver cancer cells with sorafenib enhanced intracellular ROS levels (Fig. 6H and I) and decreased MMP compared with the control group (Fig. 6J and K). Lipid peroxidation levels were markedly elevated, and the protein and mRNA expression of ferroptosis-associated genes was reduced in Hep3B cells treated with sorafenib (Fig. 6A and L-N). In summary, SSBP1 deficiency enhanced the sensitivity of liver cancer cells to sorafenib and may serve as a novel target for overcoming sorafenib resistance (Fig. 7).

Discussion

Liver cancer poses a notable clinical challenge due to the lack of early pathological indicators, which complicates diagnosis (49). This, combined with limited treatment options, contributes to high morbidity and mortality rates (1-4).

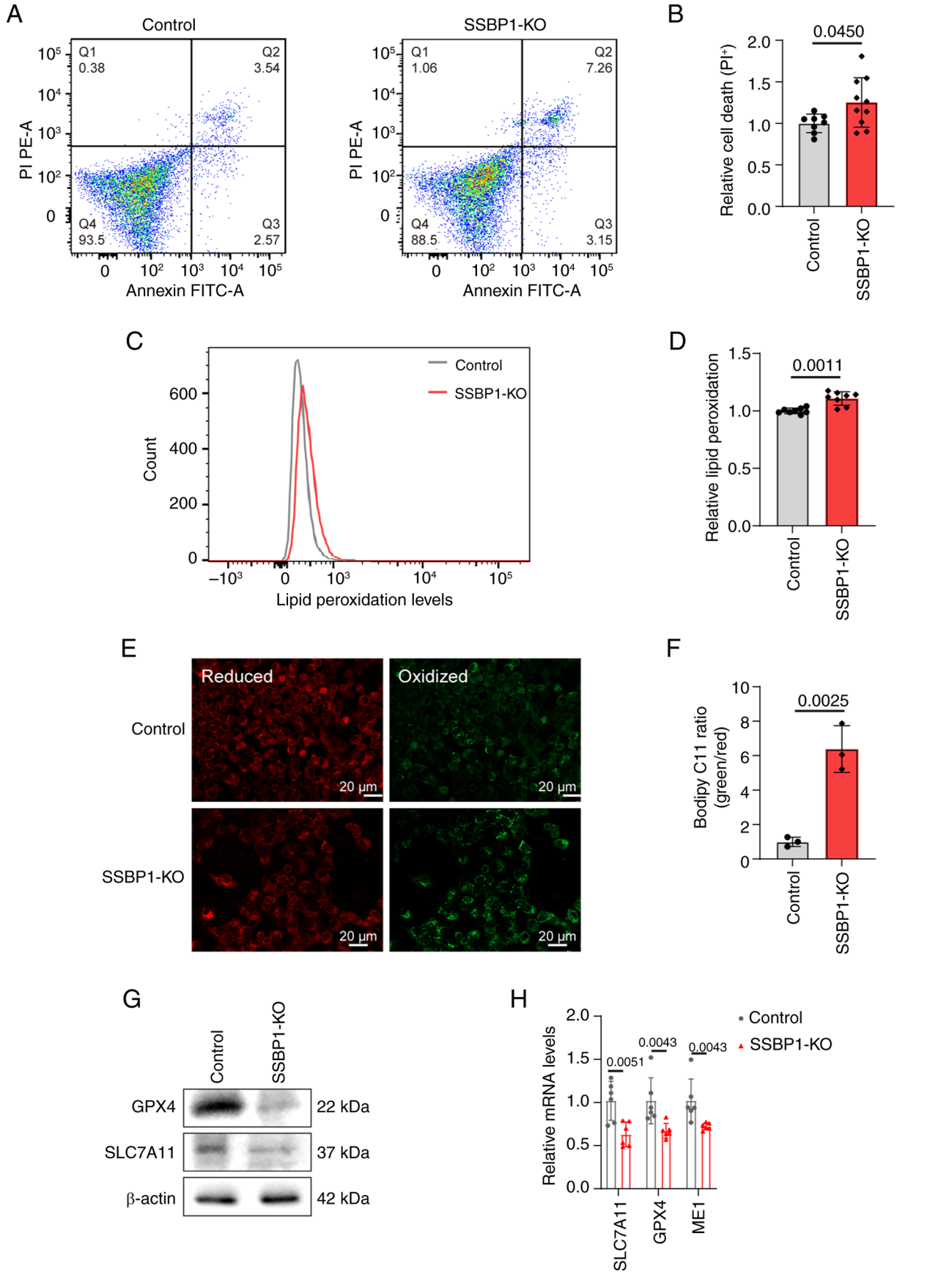

Figure 5. SSBP1 deficiency triggers ferroptosis in liver cancer cells. (A) Flow cytometry was performed to analyze (B) relative death level (PI^+) in control and *SSBP1*-KO Hep3B cells (n=8-10). (C) Flow cytometry was applied to analyze (D) C11-BODIPY levels of control and *SSBP1*-KO Hep3B cells (n=8). (E) Fluorescence images of C11-BODIPY-stained Hep3B cells. (F) Relative fluorescence intensity (n=3). Scale bar, 20 μm. Magnification, x200. (G) Western blotting of ferroptosis-associated proteins in Control and SSBP1-KO Hep3B cells. (H) mRNA expression of ferroptosis-associated genes in Control and SSBP1-KO Hep3B cells (n=6). SSBP1-KO, SSBP1 (single-stranded DNA binding protein 1) knockout; C11-BODIPY, 11-carbon-substituted boron dipyrromethene; GPX4, glutathione peroxidase 4; SLC7A11, solute carrier family 7 member 11; ME1, malic enzyme 1.

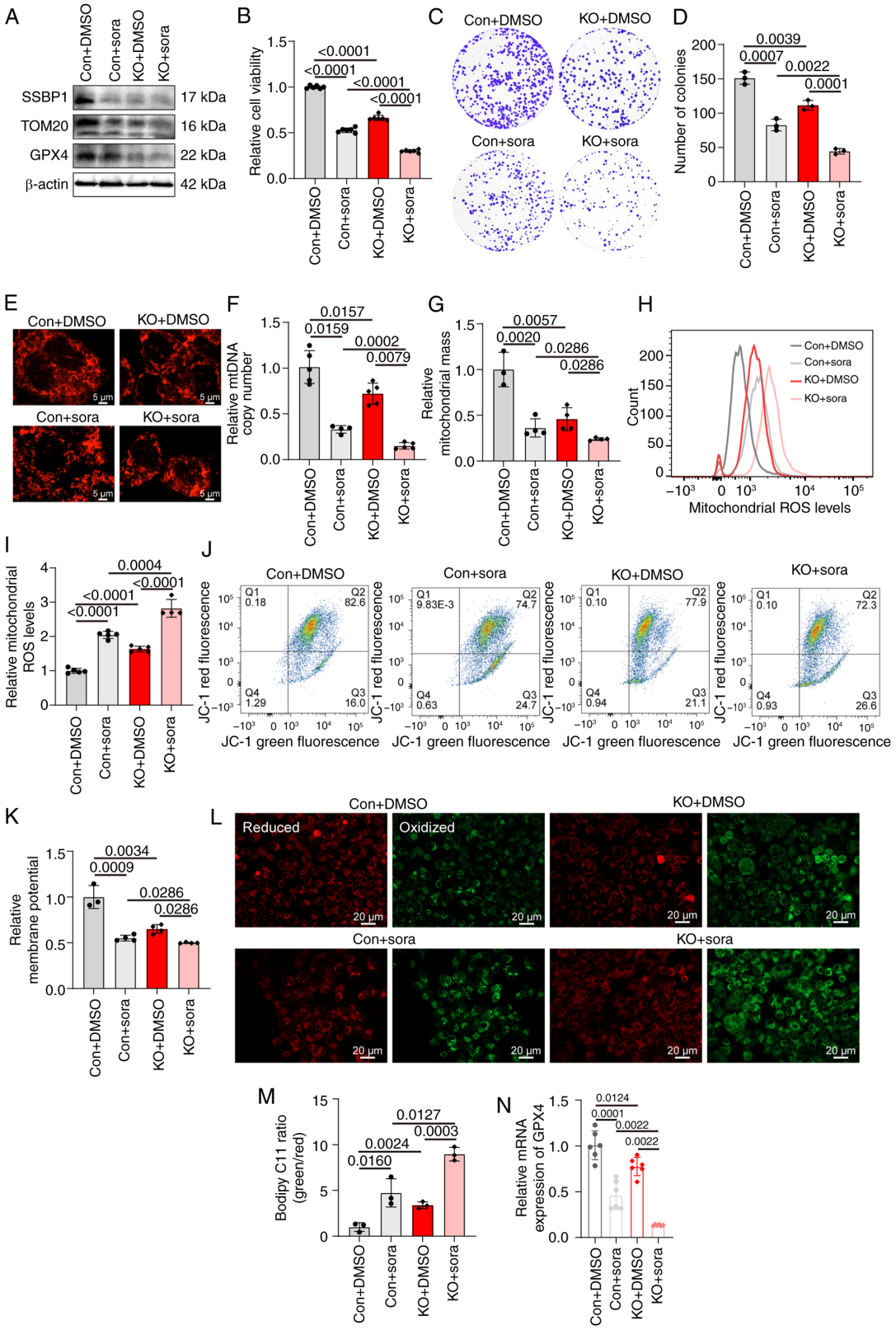

Figure 6. SSBP1 deficiency enhances the effect of sora treatment. (A) Expression of SSBP1, TOM20 and GPX4 in Con and SSBP1-KO Hep3B cells with or without sora treatment. (B) MTT assay showed the relative viability of Con and SSBP1-KO Hep3B cells with or without sora treatment (n=6). (C) Representative colony formation assay showing proliferation capacity of Hep3B cells with SSBP1 KO in the presence or absence of sora treatment. (D) Colony formation capacity (n=3). (E) Immunofluorescence was performed to detect the mitochondrial morphology in Hep3B cells following SSBP1 KO in the presence or absence of sora. Scale bar, 5 μm. Magnification, x630. (F) qPCR was used to analyze the mtDNA copy number of Con and SSBP1-KO Hep3B cells with or without sora treatment (n=4-5). Flow cytometry was employed to analyze (G) mitochondrial mass (n=3-4) and (H) ROS levels (n=4-5) of Con and SSBP1-KO Hep3B cells with or without sora treatment. (I) ROS levels in Con and SSBP1-KO Hep3B cells with or without sora (n=4-5). (J) Flow cytometry was performed to analyze (K) MMP of Control and SSBP1-KO Hep3B cells with or without sora (n=3-4). (L) Fluorescence images of C11-BODIPY-stained Hep3B cells. (M) Relative fluorescence intensity was quantified by ImageJ software (n=3). Scale bar, 20 μm. Magnification, x200. (N) mRNA expression of ferroptosis-associated gene GPX4 in Con and SSBP1-KO Hep3B cells in the presence or absence of sora (n=6). TOM20, translocase of the outer mitochondrial membrane 20; GPX4, glutathione peroxidase 4; SSBP1-KO, SSBP1 (single-stranded DNA binding protein 1) knockout; mtDNA, mitochondrial DNA; Con, control; sora, sorafenib.

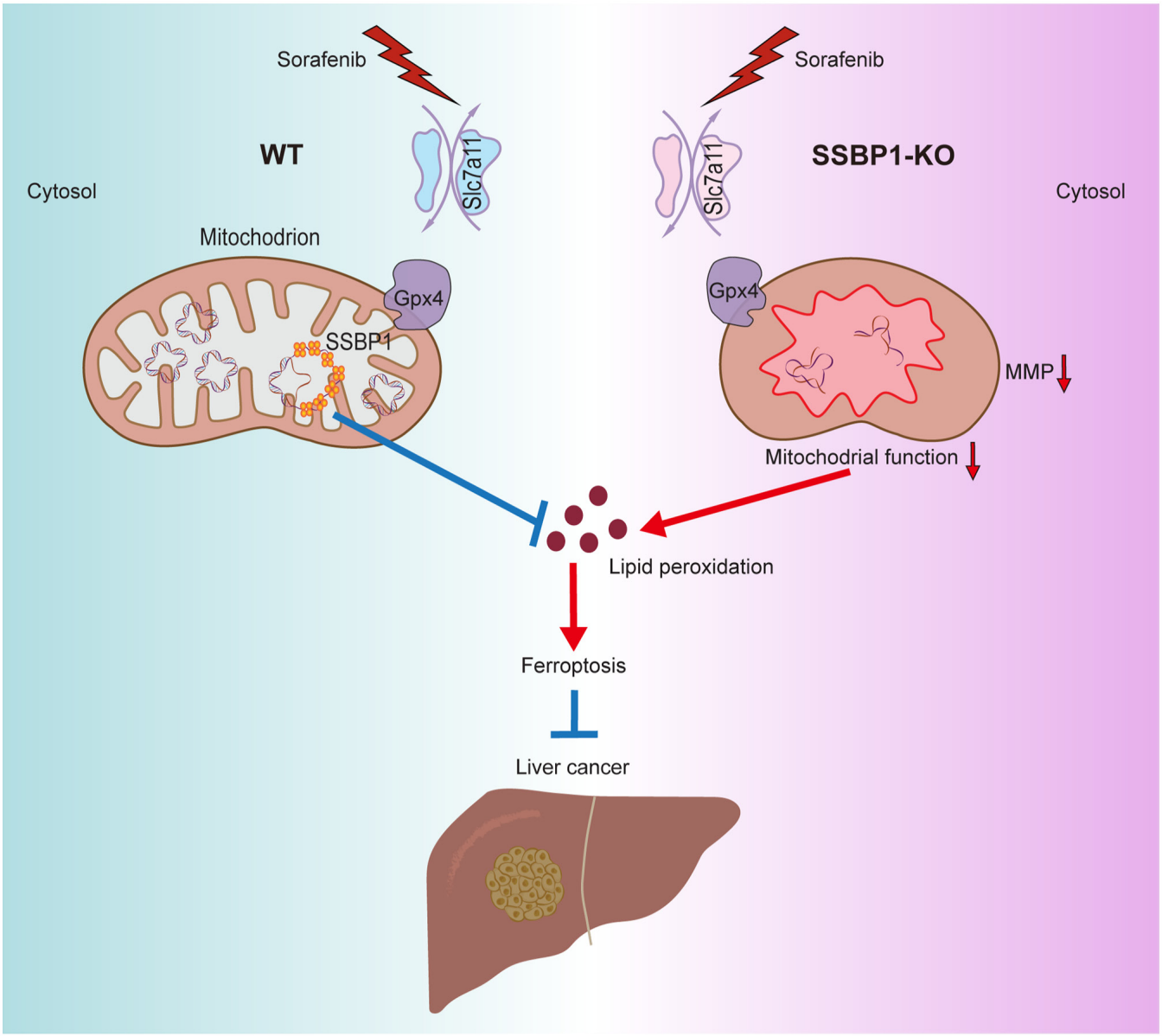

Figure 7. SSBP1 deficiency enhances liver cancer cell sensitivity to sorafenib. SSBP1 deficiency impairs mitochondrial function and exacerbates lipid peroxidation in liver cancer cells, sensitizing them to sorafenib-induced ferroptosis. SSBP1-KO-driven mitochondrial dysfunction and cytosolic/mitochondrial lipid peroxide accumulation leads to diminished GPX4 and SLC7A11 activity. These alterations amplify ferroptosis under sorafenib treatment, underscoring SSBP1 loss as a key determinant of sorafenib sensitivity in liver cancer by disrupting redox homeostasis and mitochondrial integrity. MMP, mitochondrial membrane potential; SSBP1-KO, single-stranded DNA binding protein 1-knockout; GPX4, glutathione peroxidase 4; SLC7A11, solute carrier family 7 member 11; WT, wildtype.

Furthermore, the efficacy of the currently available treatment strategies remains unsatisfactory (49). Therefore, the identification of novel targets and biomarkers to improve the clinical prognosis of patients with liver cancer is key. In the present study, SSBP1 was identified as a promising therapeutic target for liver cancer. SSBP1 was significantly upregulated in tumor compared with adjacent healthy liver tissue. Analysis of TCGA data revealed that patients with liver cancer with high SSBP1 expression displayed reduced overall survival. SSBP1, a single-stranded DNA-binding protein, serves a key role in several cellular processes including nuclear DNA replication, repair, recombination, and mitochondrial genome maintenance. In cancer, its expression and activity are typically altered, thus affecting tumor cell proliferation and metastasis (24,25,28). Previous studies demonstrated that SSBP1 is highly expressed in certain types of cancer (such as lung adenocarcinoma) and involved in tumor occurrence and development (49-52). However, the role of SSBP1 in liver cancer remains unclear. Ohmori *et al* (53) cloned the single-stranded DNA-binding protein in 1996, highlighting its key role in the maximal expression of the thyroid-stimulating hormone (TSH) receptor and TSH-induced negative regulation, thus suggesting that SSBP1 serves a potential role in cellular signaling regulation. However, its function in liver cancer remains to be explored. The present results showed that SSBP1 was highly expressed in tumor compared with adjacent healthy liver tissues. TCGA dataset revealed that patients with liver cancer highly expressing SSBP1 had decreased overall survival, which was

consistent with the research findings of Yang *et al* (54) in lung adenocarcinoma. These findings indicated that high SSBP1 expression may serve as a potential indicator of poor prognosis. In terms of cell functions, the results demonstrated that SSBP1 deficiency suppressed the proliferation and migration of liver cancer cells, while SSBP1 overexpression displayed the opposite effects. These findings were consistent with the known proliferative and metastasis-promoting effects of SSBP1 on other types of cancer, which were verified in liver cancer cell lines (28).

As a key regulator of the mitochondrial genome, SSBP1 serves a role in maintaining mitochondrial function, modulating metabolism and responding to DNA damage (55-57). Additionally, SSBP1 is involved in the mitochondrial unfolded protein response (58). Comparative mitochondrial proteomic analysis of patients with liver cancer provides insights for exploring mitochondria-associated protein alterations in liver cancer (59). A previous study revealed that SSBP1 downregulation decreases mtDNA content and perturbs mitochondrial energy function in glioblastoma cells (43). In line with these findings, elevated mtDNA copy number was recorded in liver cancer tissue with high SSBP1 expression. In addition, SSBP1 knockout in liver cancer cells decreased mitochondrial number, mtDNA copy number and the levels of mitochondrial proteins, and increased migration to the nucleus. Additionally, SSBP1-deficient cells exhibited increased mitochondrial ROS levels and decreased MMP, indicating mitochondrial damage. The aforementioned findings aligned with those of previous studies supporting the role of SSBP1 in maintaining mitochondrial function and further highlighted the role of SSBP1 in regulating mitochondrial function in liver cancer cells (27,28). Mitochondria are considered the primary source of intracellular ROS and serve a crucial role in governing ferroptosis (44). To investigate the potential association between SSBP1 and ferroptosis, ferroptosis was assessed utilizing C11-BODIPY fluorescence staining and by detecting the expression of ferroptosis-related genes in liver cancer cells. Notably, ferroptosis was significantly induced in liver cancer cells following SSBP1 knockout. This finding was consistent with those of previous studies indicating that SSBP1 regulates ferroptosis via p53 signaling in glomerular podocyte injury (45,60). Overall, the aforementioned findings demonstrate the mechanism underlying the effects of SSBP1 on regulating ferroptosis in liver cancer.

Inducing tumor cell death via pharmacological, genetic and other interventional modalities is a fundamental strategy for treating cancer (61). Numerous types of cell death have been identified, including apoptosis, necrosis, autophagy and ferroptosis (62). Ferroptosis is characterized by uncontrolled lipid peroxidation. Therefore, ferroptosis is considered a novel tumor-suppression mechanism (63-65). As the liver is susceptible to oxidative damage, ferroptosis has garnered increasing attention within the realm of liver disease, particularly liver cancer (44,48). Previous studies have primarily focused on sorafenib-induced ferroptosis and its potential targets both *in vivo* and/or *in vitro* (66-68). Although sorafenib is a multi-kinase inhibitor that is considered the first-line systemic therapy for patients with advanced liver cancer, drug resistance can hamper its broad application (9). Therefore, it has been hypothesized that genes that inhibit ferroptosis contribute to sorafenib resistance (69). The present study revealed that SSBP1 knockout markedly enhanced liver cancer cell ferroptosis and concurrently inhibited cell proliferation when combined with sorafenib treatment. In addition, mitochondrial dysfunction and increased ROS levels induced by SSBP1 knockout may collectively contribute to sorafenib-induced ferroptosis in liver cancer. This implied that SSBP1 regulates ferroptosis sensitivity through multiple pathways. On one hand, the burst of mitochondrial ROS may directly initiate lipid peroxidation chain reactions. On the other hand, mitochondrial dysfunction may promote the release of mtDNA, thus activating the cGAS (cyclic GMP-AMP synthase)/STING pathway and facilitating ferroptosis in liver cancer cells (70). SSBP1 forms a complex with heat shock factor 1 that translocates into the nucleus to regulate mitochondrial protein import (71). Therefore, SSBP1 knockout could disrupt the mitochondrial localization of GPX4, thus impairing GSH redox cycling, a key antioxidant defense mechanism against lipid peroxidation, and enhancing ferroptosis. Overall, the aforementioned findings underscore the key role of SSBP1 in modulating cell survival and response to therapy, underlining its potential as a target for developing more effective treatment strategies for liver cancer.

While the present study demonstrates that SSBP1 influences sorafenib efficacy via ferroptosis, it did not include liver cancer specimens, and further studies are needed to investigate the role of SSBP1 in other signaling pathways, which may reveal broader therapeutic implications.

Overall, the mechanism by which SSBP1 regulates tumor cell proliferation and sorafenib resistance in liver cancer was elucidated. SSBP1 promoted the malignant progression of liver cancer via suppressing ferroptosis. The present data provided novel insights into the critical role of SSBP1 as a potential target for liver cancer therapy.

Acknowledgements

Not applicable.

Funding

The present study was supported by the Scientific Research Program of Tianjin Education Commission (Natural Science; grant no. 2023KJ037).

Availability of data and materials

The data generated in the present study may be requested from the corresponding author.

Authors' contributions

ZW and LZ conceived the study. SL, XY and HG performed the experiments, analyzed data and wrote and revised the manuscript. XH, DW, QZ, JX, JZ and LZ analyzed and interpreted data. All authors have read and approved the final manuscript. SL, LZ and ZW take responsibility for the integrity of data analysis. ZW and LZ confirm the authenticity of all the raw data.

Ethics approval and consent to participate

The animal experiments were approved by the Animal Care and Use Committee of Tianjin Medical University (approval no. TMUaMEC2024050; Tianjin, China).

Patient consent for publication

Not applicable.

Competing interests

The authors declare that they have no competing interests.

References

1. Bray F, Laversanne M, Sung H, Ferlay J, Siegel RL, Soerjomataram I and Jemal A: Global cancer statistics 2022: GLOBOCAN estimates of incidence and mortality worldwide for 36 cancers in 185 countries. CA Cancer J Clin 74: 229-263, 2024.
2. Li M, He H, Zhao X, Guan M, Khattab N, Elshishiney G, You H and Hu Y: Trends in burden of liver cancer and underlying etiologies in China, 1990-2021. Lancet Regional Health-Western Pacific 55: 101385, 2025.
3. Rumgay H, Arnold M, Ferlay J, Lesi O, Cabasag CJ, Vignat J, Laversanne M, McGlynn KA and Soerjomataram I: Global burden of primary liver cancer in 2020 and predictions to 2040. J Hepatol 77: 1598-1606, 2022.
4. Villanueva A: Hepatocellular carcinoma. N Engl J Med 380: 1450-1462, 2019.
5. Singal AG, Kanwal F and Llovet JM: Global trends in hepatocellular carcinoma epidemiology: Implications for screening, prevention and therapy. Nat Rev Clin Oncol 20: 864-884, 2023.
6. Zhang H, Zhang W, Jiang L and Chen Y: Recent advances in systemic therapy for hepatocellular carcinoma. Biomark Res 10: 3, 2022.
7. Llovet JM, Ricci S, Mazzaferro V, Hilgard P, Gane E, Blanc JF, de Oliveira AC, Santoro A, Raoul JL, Forner A, *et al*: Sorafenib in advanced hepatocellular carcinoma. N Engl J Med 359: 378-390, 2008.
8. Guo L, Hu C, Yao M and Han G: Mechanism of sorafenib resistance associated with ferroptosis in HCC. Front Pharmacol 14: 1207496, 2023.
9. Dixon SJ, Patel DN, Welsch M, Skouta R, Lee ED, Hayano M, Thomas AG, Gleason CE, Tatonetti NP, Slusher BS, *et al*: Pharmacological inhibition of cystine-glutamate exchange induces endoplasmic reticulum stress and ferroptosis. eLife 3: e02523, 2014.
10. Jurisic V, Bumbasirevic V, Konjevic G, Djuricic B and Spuzic I: TNF-alpha induces changes in LDH isotype profile following triggering of apoptosis in PBL of non-Hodgkin's lymphomas. Ann Hematol 83: 84-91, 2004.
11. Dixon SJ, Lemberg KM, Lamprecht MR, Skouta R, Zaitsev EM, Gleason CE, Patel DN, Bauer AJ, Cantley AM, Yang WS, *et al*: Ferroptosis: An iron-dependent form of nonapoptotic cell death. Cell 149: 1060-1072, 2012.
12. Stockwell BR, Friedmann Angeli JP, Bayir H, Bush AI, Conrad M, Dixon SJ, Fulda S, Gascon S, Hatzios SK, Kagan VE, *et al*: Ferroptosis: A regulated cell death nexus linking metabolism, redox biology, and disease. Cell 171: 273-285, 2017.
13. Zhou Q, Meng Y, Li D, Yao L, Le J, Liu Y, Sun Y, Zeng F, Chen X and Deng G: Ferroptosis in cancer: From molecular mechanisms to therapeutic strategies. Signal Transduct Target Ther 9: 55, 2024.
14. Fulda S, Galluzzi L and Kroemer G: Targeting mitochondria for cancer therapy. Nat Rev Drug Discov 9: 447-464, 2010.
15. Wallace DC: Mitochondria and cancer. Nat Rev Cancer 12: 685-698, 2012.
16. Eckl EM, Ziegemann O, Krumwiede L, Fessler E and Jae LT: Sensing, signaling and surviving mitochondrial stress. Cell Mol Life Sci 78: 5925-5951, 2021.
17. Kasahara A and Scorrano L: Mitochondria: From cell death executioners to regulators of cell differentiation. Trends Cell Biol 24: 761-770, 2014.
18. Senft D and Ronai ZA: Regulators of mitochondrial dynamics in cancer. Curr Opin Cell Biol 39: 43-52, 2016.
19. Kashatus JA, Nascimento A, Myers LJ, Sher A, Byrne FL, Hoehn KL, Counter CM and Kashatus DF: Erk2 phosphorylation of Drp1 promotes mitochondrial fission and MAPK-driven tumor growth. Mol Cell 57: 537-551, 2015.
20. Bianchi NO, Bianchi MS and Richard SM: Mitochondrial genome instability in human cancers. Mutat Res 488: 9-23, 2001.
21. Yang Y, Karakhanova S, Hartwig W, D'Haese JG, Philippov PP, Werner J and Bazhin AV: Mitochondria and mitochondrial ROS in cancer: Novel targets for anticancer therapy. J Cell Physiol 231: 2570-2581, 2016.
22. Leao Barros MB, Pinheiro DDR and Borges BDN: Mitochondrial DNA Alterations in Glioblastoma (GBM). Int J Mol Sci 22: 5855, 2021.
23. Arakaki N, Nishihama T, Kohda A, Owaki H, Kuramoto Y, Abe R, Kita T, Suenaga M, Himeda T, Kuwajima M, *et al*: Regulation of mitochondrial morphology and cell survival by Mitogenin I and mitochondrial single-stranded DNA binding protein. Biochim Biophys Acta 1760: 1364-1372, 2006.
24. Oliveira MT and Kaguni LS: Functional roles of the N- and C-terminal regions of the human mitochondrial single-stranded DNA-binding protein. PLoS One 5: e15379, 2010.
25. Li Y, Bolderson E, Kumar R, Muniandy PA, Xue Y, Richard DJ, Seidman M, Pandita TK, Khanna KK and Wang W: HSSB1 and hSSB2 form similar multiprotein complexes that participate in DNA damage response. J Biol Chem 284: 23525-23531, 2009.
26. Zelinger L and Swaroop A: SSBP1 faux pas in mitonuclear tango causes optic neuropathy. J Clin Invest 130: 62-64, 2020.
27. Wang Y, Hu L, Zhang X, Zhao H, Xu H, Wei Y, Jiang H, Xie C, Zhou Y and Zhou F: Downregulation of mitochondrial single stranded DNA binding protein (SSBP1) induces mitochondrial dysfunction and increases the radiosensitivity in Non-small cell lung cancer cells. J Cancer 8: 1400-1409, 2017.
28. Su J, Li Y, Liu Q, Peng G, Qin C and Li Y: Identification of SSBP1 as a ferroptosis-related biomarker of glioblastoma based on a novel mitochondria-related gene risk model and in vitro experiments. J Transl Med 20: 440, 2022.
29. Zhang T, Cui Y, Wu Y, Meng J, Han L, Zhang J, Zhang C, Yang C, Chen L, Bai X, *et al*: Mitochondrial GCN5L1 regulates glutaminase acetylation and hepatocellular carcinoma. Clin Transl Med 12: e852, 2022.
30. Cancer Genome Atlas Research Network. Electronic address: wheeler@bcm.edu; Cancer Genome Atlas Research Network: Comprehensive and integrative genomic characterization of hepatocellular carcinoma. Cell 169: 1327-1341.23, 2017.
31. Rath S, Sharma R, Gupta R, Ast T, Chan C, Durham TJ, Goodman RP, Grabarek Z, Haas ME, Hung WHW, *et al*: MitoCarta3.0: An updated mitochondrial proteome now with sub-organelle localization and pathway annotations. Nucleic Acids Res 49: D1541-D1547, 2021.
32. Zhou X, Liu C, Zeng H, Wu D and Liu L: Identification of a thirteen-gene signature predicting overall survival for hepatocellular carcinoma. Biosci Rep 41: BSR20202870, 2021.
33. Zhou Y, Zhou B, Pache L, Chang M, Khodabakhshi AH, Tanaseichuk O, Benner C and Chanda SK: Metascape provides a biologist-oriented resource for the analysis of systems-level datasets. Nat Commun 10: 1523, 2019.
34. Roessler S, Jia HL, Budhu A, Forgues M, Ye QH, Lee JS, Thorgeirsson SS, Sun Z, Tang ZY, Qin LX, *et al*: A unique metastasis gene signature enables prediction of tumor relapse in early-stage hepatocellular carcinoma patients. Cancer Res 70: 10202-10212, 2010.
35. Sun Q, Liu P, Long B, Zhu Y and Liu T: Screening of significant biomarkers with poor prognosis in hepatocellular carcinoma via bioinformatics analysis. Medicine (Baltimore) 99: e21702, 2020.
36. Vazquez Salgado AM, Preziosi ME, Yin D, Holczbauer A, Zahm AM, Erez N, Kieckhaefer J, Ackerman D, Gade TP, Kaestner KH, *et al*: In vivo screen identifies liver X receptor alpha agonism potentiates sorafenib killing of hepatocellular carcinoma. Gastro Hep Adv 1: 905-908, 2022.
37. van Malenstein H, Dekervel J, Verslype C, Van Cutsem E, Windmolders P, Nevens F and van Pelt J: Long-term exposure to sorafenib of liver cancer cells induces resistance with epithelial-to-mesenchymal transition, increased invasion and risk of rebound growth. Cancer Lett 329: 74-83, 2013.
38. Barrett T, Wilhite SE, Ledoux P, Evangelista C, Kim IF, Tomashevsky M, Marshall KA, Phillippy KH, Sherman PM, Holko M, *et al*: NCBI GEO: Archive for functional genomics data sets-update. Nucleic Acids Res 41: D991-D995, 2013.

39. Li T, Fu J, Zeng Z, Cohen D, Li J, Chen Q, Li B and Liu XS: TIMER2.0 for analysis of tumor-infiltrating immune cells. Nucleic Acids Res 48: W509-W514, 2020.
40. Chandrashekar DS, Bashel B, Balasubramanya SAH, Creighton CJ, Ponce-Rodriguez I, Chakravarthi B and Varambally S: UALCAN: A portal for facilitating tumor subgroup gene expression and survival analyses. Neoplasia 19: 649-658, 2017.
41. Gyorffy B: Integrated analysis of public datasets for the discovery and validation of survival-associated genes in solid tumors. Innovation (Camb) 5: 100625, 2024.
42. Livak KJ and Schmittgen TD: Analysis of relative gene expression data using real-time quantitative PCR and the 2(-Delta Delta C(T)) method. Methods 25: 402-408, 2001.
43. Radenkovic S, Konjevic G, Gavrilovic D, Stojanovic-Rundic S, Plesinac-Karapandzic V, Stevanovic P and Jurisic V: pSTAT3 expression associated with survival and mammographic density of breast cancer patients. Pathol Res Pract 215: 366-372, 2019.
44. Hu X, Zhang P, Li S, Zhang J, Wang D, Wang Z, Zhu L and Wang L: Mitochondrial GCN5L1 acts as a novel regulator for iron homeostasis to promote sorafenib sensitivity in hepatocellular carcinoma. J Transl Med 22: 593, 2024.
45. Scherbakov AM, Vorontsova SK, Khamidullina AI, Mrdjanovic J, Andreeva OE, Bogdanov FB, Salnikova DI, Jurisic V, Zavarzin IV and Shirinian VZ: Novel pentacyclic derivatives and benzylidenes of the progesterone series cause anti-estrogenic and antiproliferative effects and induce apoptosis in breast cancer cells. Invest New Drugs 41: 142-152, 2023.
46. Radenkovic N, Milutinovic M, Nikodijevic D, Jovankic J and Jurisic V: Sample preparation of adherent cell lines for flow cytometry: Protocol optimization-our experience with SW-480 colorectal cancer cell line. Indian J Clin Biochem 40: 74-79, 2025.
47. Hernansanz-Agustin P and Enriquez JA: Generation of reactive oxygen species by mitochondria. Antioxidants (Basel) 10: 415, 2021.
48. Sun K, Zhi Y, Ren W, Li S, Zhou X, Gao L and Zhi K: The mitochondrial regulation in ferroptosis signaling pathway and its potential strategies for cancer. Biomed Pharmacother 169: 115892, 2023.
49. Llovet JM, Kelley RK, Villanueva A, Singal AG, Pikarsky E, Roayaie S, Lencioni R, Koike K, Zucman-Rossi J and Finn RS: Hepatocellular carcinoma. Nat Rev Dis Primers 7: 6, 2021.
50. Huang J and Xie ZF: Identification of SSBP1 as a prognostic marker in human lung adenocarcinoma using bioinformatics approaches. Math Biosci Eng 19: 3022-3035, 2022.
51. Li Q, Qu F, Li R, He X, Zhai Y, Chen W and Zheng Y: A functional polymorphism of SSBP1 gene predicts prognosis and response to chemotherapy in resected gastric cancer patients. Oncotarget 8: 110861-110876, 2017.
52. Xu S, Feng Z, Zhang M, Wu Y, Sang Y, Xu H, Lv X, Hu K, Cao J, Zhang R, *et al*: hSSB1 binds and protects p21 from ubiquitin-mediated degradation and positively correlates with p21 in human hepatocellular carcinomas. Oncogene 30: 2219-2229, 2011.
53. Ohmori M, Ohta M, Shimura H, Shimurat Y, Suzuki K and Kohn LD: Cloning of the single strand DNA-binding protein important for maximal expression and thyrotropin (TSH)-induced negative regulation of the TSH receptor. Mol Endocrinol 10: 1407-1424, 1996.
54. Yang X, Ma B, Liu Y, Zhou J, Guo J, Peng Y, Bai Y, Wu J and Hu D: SSBP1 positively regulates RRM2, affecting epithelial mesenchymal transition and cell cycle arrest in human lung adenocarcinoma cells. Cell Signal 127: 111552, 2025.
55. Morin JA, Cerron F, Jarillo J, Beltran-Heredia E, Ciesielski GL, Arias-Gonzalez JR, Kaguni LS, Cao FJ and Ibarra B: DNA synthesis determines the binding mode of the human mitochondrial single-stranded DNA-binding protein. Nucleic Acids Res 45: 7237-7248, 2017.
56. Richard DJ, Bolderson E, Cubeddu L, Wadsworth RI, Savage K, Sharma GG, Nicolette ML, Tsvetanov S, McIlwraith MJ, Pandita RK, *et al*: Single-stranded DNA-binding protein hSSB1 is critical for genomic stability. Nature 453: 677-681, 2008.
57. Sykora P, Kanno S, Akbari M, Kulikowicz T, Baptiste BA, Leandro GS, Lu H, Tian J, May A, Becker KA, *et al*: DNA Polymerase beta participates in mitochondrial DNA repair. Mol Cell Biol 37: e00237-17, 2017.
58. Zhang S, Guo H, Wang H, Liu X, Wang M, Liu X, Fan Y and Tan K: A novel mitochondrial unfolded protein response-related risk signature to predict prognosis, immunotherapy and sorafenib sensitivity in hepatocellular carcinoma. Apoptosis 29: 768-784, 2024.
59. Ye Y, Huang A, Huang C, Liu J, Wang B, Lin K, Chen Q, Zeng Y, Chen H, Tao X, *et al*: Comparative mitochondrial proteomic analysis of hepatocellular carcinoma from patients. Proteomics Clin Appl 7: 403-415, 2013.
60. Wu WY, Wang ZX, Li TS, Ding XQ, Liu ZH, Yang J, Fang L and Kong LD: SSBP1 drives high fructose-induced glomerular podocyte ferroptosis via activating DNA-PK/p53 pathway. Redox Biol 52: 102303, 2022.
61. Jurisic V, Bogdanovic G, Srdic T, Jakimov D, Mrdjanovic J, Baltic M and Baltic VV: Modulation of TNF-alpha activity in tumor PC cells using anti-CD45 and anti-CD95 monoclonal antibodies. Cancer Lett 214: 55-61, 2004.
62. Tang D, Kang R, Berghe TV, Vandenabeele P and Kroemer G: The molecular machinery of regulated cell death. Cell Res 29: 347-364, 2019.
63. Li D, Wang Y, Dong C, Chen T, Dong A, Ren J, Li W, Shu G, Yang J, Shen W, *et al*: CST1 inhibits ferroptosis and promotes gastric cancer metastasis by regulating GPX4 protein stability via OTUB1. Oncogene 42: 83-98, 2023.
64. Li H, Yu K, Hu H, Zhang X, Zeng S, Li J, Dong X, Deng X, Zhang J and Zhang Y: METTL17 coordinates ferroptosis and tumorigenesis by regulating mitochondrial translation in colorectal cancer. Redox Biol 71: 103087, 2024.
65. Yuan S, Xi S, Weng H, Guo MM, Zhang JH, Yu ZP, Zhang H, Yu Z, Xing Z, Liu MY, *et al*: YTHDC1 as a tumor progression suppressor through modulating FSP1-dependent ferroptosis suppression in lung cancer. Cell Death Differ 30: 2477-2490, 2023.
66. Lachaier E, Louandre C, Godin C, Saidak Z, Baert M, Diouf M, Chauffert B and Galmiche A: Sorafenib induces ferroptosis in human cancer cell lines originating from different solid tumors. Anticancer Res 34: 6417-6422, 2014.
67. Li Y, Xia J, Shao F, Zhou Y, Yu J, Wu H, Du J and Ren X: Sorafenib induces mitochondrial dysfunction and exhibits synergistic effect with cysteine depletion by promoting HCC cells ferroptosis. Biochem Biophys Res Commun 534: 877-884, 2021.
68. Louandre C, Marcq I, Bouhlal H, Lachaier E, Godin C, Saidak Z, Francois C, Chatelain D, Debuysscher V, Barbare JC, *et al*: The retinoblastoma (Rb) protein regulates ferroptosis induced by sorafenib in human hepatocellular carcinoma cells. Cancer Lett 356: 971-977, 2015.
69. Guo M, Chen S, Sun J, Xu R, Qi Z, Li J, Zhou L, Fang Y, Liu T and Xia J: PIP5K1A suppresses ferroptosis and induces sorafenib resistance by stabilizing NRF2 in hepatocellular carcinoma. Adv Sci (Weinh): e04372, 2025 doi: 10.1002/advs.202504372 (Epub ahead of print).
70. Zhao X, Yu M, Zhao Y, Zheng Y, Meng L, Du K, Xie Z, Lv H, Zhang W, Liu J, *et al*: Circulating cell-free mtDNA release is associated with the activation of cGAS-STING pathway and inflammation in mitochondrial diseases. J Neurol 269: 4985-4996, 2022.
71. Tan K, Fujimoto M, Takii R, Takaki E, Hayashida N and Nakai A: Mitochondrial SSBP1 protects cells from proteotoxic stresses by potentiating stress-induced HSF1 transcriptional activity. Nat Commun 6: 6580, 2015.